Basic structure of the kinked monatomic steps on the Si(001) surface

Ja-Yong Koo*
Korea Research Institute of Standards and Science, P.O. Box 102, Yusong, Taejon 305-600, Korea

Jae-Yel Yi
Department of Physics, Dong-A University, Hadan-Dong, Saha-Gu, Pusan 604-714, Korea

Chanyong Hwang, Dal-Hyun Kim, Geunseop Lee, and Sekyung Lee
Korea Research Institute of Standards and Science, P.O. Box 102, Yusong, Taejon 305-600, Korea
(Received 4 December 1997)

The atomic structure of monatomic steps on Si(001) is investigated with scanning tunneling microscopy. On the upper terrace of the S_B step the existence of kinks induces a local $p(2\times2)$ structure with the direction to the center of the step. The structure of the S_B step is correlated to that of the S_A step through the kinks and is determined by the boundary conditions imposed by the S_A step. The atomic structure of the steps is also correlated with the zigzag buckling along the dimer row of the lower terrace through the subsurface interaction. The formation of various structures observed near the steps is explained by the simple geometric rule based on the bonding characteristics. [S0163-1829(98)01216-8]

The Si atoms on the Si(001) surface form symmetric-appearing dimers, resulting in the 2×1 reconstruction, at room temperature.[1] When one or two of the dimers in the dimer row are permanently buckled in one direction by asymmetric defects or step edges, the neighboring dimers in the dimer row are always buckled successively in a zigzag form and the bucklings decay out far from the buckling source at room temperature.[2] The zigzag buckling is supposed to be an intrinsic property of a dimer row to accommodate the strains of the second-layer atoms supporting the dimer row,[3,4] and/or to lower the Coulombic potential between the charged buckled atoms of the dimers.[5,6] At low temperatures the number of buckled dimer rows increases at the expense of the symmetric dimer rows. Most of the surfaces are covered by the $c(4\times2)$ structure, but the $p(2\times2)$ structure is found only in the antiphase boundaries.[7–9] Hence it is generally believed that $c(4\times2)$ has a lower formation energy than $p(2\times2)$ on the Si(001) surface even though theoretical calculations predicted that these states are almost degenerate within the accuracy of the calculations.[10–12]

The step on the Si(001) surface is one of the most abundant intrinsic defects. It causes inhomogeneities on the clean surface and affects the nucleation and growth in the epitaxy.[13–19] The monatomic step on the Si(001) surface is classified into two types of steps: S_A and S_B.[13] For the S_A step, only one configuration is experimentally found, where the up atoms of the step edge in the upper terrace are aligned with the center of the dimer row in the lower terrace and the down atoms are aligned with the gap between the dimer rows in the lower terrace. The other variant with the opposite buckling to the S_A step edge has not been observed in experiments.[1] Three configurations of the S_B step have been experimentally observed: rebonded, nonrebonded, and split. On the well-prepared clean Si(001) surface, the fundamental S_B step edge is a rebonded one. When the surface is under a tensional stress due to the presence of vacancy defects, the rebonded one is transformed into a split one, which is a combination of a nonrebonded step with an additional dimer on the adjacent dimer row of the lower terrace. The nonrebonded type appears only in a special environment where a free movement and/or a supply of atoms are restricted.[19] Since every step has a finite width, it contains kinks inevitably at both ends. The structure at kink sites is influenced by a strong asymmetric environment, resulting in a variety of local structures along the S_B steps.

In this paper we investigate the atomic structure of the kinked monatomic S_A and S_B steps using scanning tunneling microscopy. A simple geometric rule based on bonding characteristics is suggested to explain the formation of the various structures observed near the steps.

The experiments are performed in an ultrahigh vacuum below 3×10^{-10} Torr with a homemade scanning tunneling microscope (STM). The Si(001) samples are cut from a P-doped Si(001) wafer (10 Ω cm) and wrapped with Ta foil at both ends to prevent a direct contact with the Mo holder. Then the samples are mounted on the Mo sample holder without any wet cleaning or etching and are transferred to the STM chamber. The heating procedures are the same as previously described.[2]

Figures 1(a) and 1(b) show the filled-state STM image of Si(001)-2×1 at room temperature and the depth profiles along the buckled dimer rows whose bucklings are induced by the local point defect, respectively. The asymmetric effect due to the point defect induces the buckling of the dimer row A, which successively makes the dimer row B buckled. The magnitude of buckling of each dimer in the dimer row B is roughly proportional to that of the nearest dimer of the dimer row A as shown in the depth profiles of Fig. 1(b). The interaction between dimer rows A and B produces a local $c(4\times2)$ rather than a local $p(2\times2)$ structure.

The dimers at the S_A step edges experience the asymmetric effect due to the absence of the dimers on the lower terrace, which causes the unique permanent buckling of

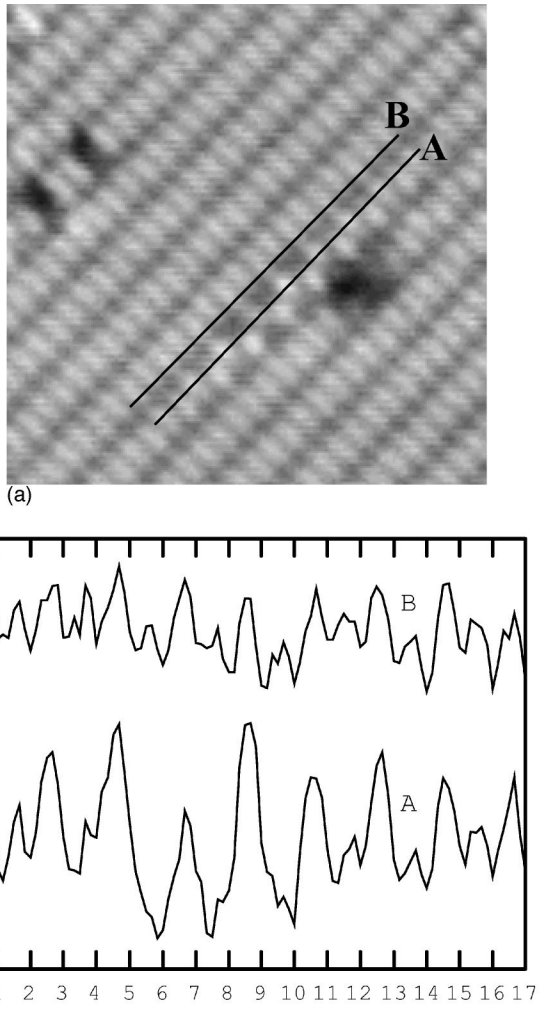

FIG. 1. (a) Filled-state STM image of the Si(001) surface. The tunneling current and sample bias voltage are 0.3 nA and -2.5 V, respectively. (b) Two depth profiles along the lines on the edges of dimer rows A and B. The buckling of the dimer row B is induced by the dimer row A resulting in the formation of a local $c(4\times2)$ structure. The unit in the horizontal axis is 3.84 Å of the surface lattice spacing on the Si(001) surface.

dimers at the edges. The direction of buckling might be determined by the bonding characteristics. A specific direction is favored to reduce the total energy.

Figure 2(a) shows the schematic atomic structure of the real S_A step edge and the other variant with the opposite buckling, which has not been observed in experiment. The main difference between the two configurations comes from the bonding structure of atoms in the third layer. The two upward bondings of the atoms A in the upper configuration in Fig. 2(a) are bent in the same direction, while the upward bondings of the atoms B in the lower configuration are twisted with respect to the two downward bondings. To reduce the strain energy, the atoms A can adjust their positions toward the bending direction. However, the twisted upward bonds of atoms B make the atoms B more difficult to adjust their positions to release the stress. The same effect is expected in the configurations of $c(4\times2)$ and $p(2\times2)$ of Fig. 2(b), that is, $c(4\times2)$ is preferred because of the bonding structure of atoms in the third layer.

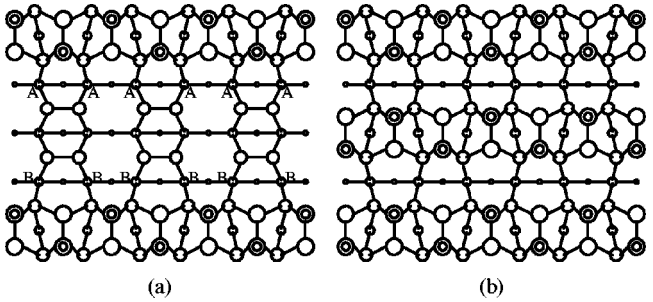

FIG. 2. (a) Schematic atomic model of two configurations of the S_A step with opposite bucklings at the step edge. Only the upper configuration appears in experiment. The smaller circles denote the atoms in the lower layer. The double circle represents the upward buckled atom of the dimer. The strains of the second-layer atoms are exaggerated in the plot. (b) Local structures of $c(4\times2)$ and $p(2\times2)$. The main difference between the two is the direction of the two upward bondings of the third-layer atoms, similar to the case of the S_A step.

Figure 3(a) shows the filled-state image of the segments of the well-aligned S_B step. The step contains two types of kink, i.e., positive and negative kinks. The positive kink (hereafter the P kink) is exposed to the open space and the negative kink (N kink) has a neighboring dimer row which is longer than the dimer rows included in the S_B step. Every well-aligned finite S_B step is bounded by two kinks, positive and/or negative. An outmost dimer at the kink is buckled toward the center of the S_B step in the filled state STM image irrespective of the type of kink as shown in Fig. 3(b). When the S_B step is wider than four dimer rows, the inner dimer row in the S_B step forms a local $p(2\times2)$ structure cooperating with the outmost dimer row terminating at the kink. Two kinks of the same segment are oppositely directed toward the center of the S_B step, resulting in the $p(2\times2)$ structures with opposite orientations at the step edges. The $p(2\times2)$ structures meet at the central part of the segment of the step, which becomes symmetric. Especially when the S_B step is composed of only two dimer rows as in Fig. 3(b), a local $c(4\times2)$ structure is constructed at the upper terrace of the S_B step irrespective of the type of the two bounding kinks. Figure 3(a) also shows the P-kink induced buckling along the corresponding dimer row in the lower terrace.[20]

The bucklings of the inner rebonded dimers at the S_B step edge in Fig. 3(a) become weak and the bucklings of dimers along the corresponding dimer rows decay out deep into the upper terrace because the asymmetric effect due to the termination of dimers of the step edge becomes weak. It implies that the dimer buckling and the formation of the $p(2\times2)$ on the upper terrace of the S_B step originates from the buckling of dimers at the kinks.

We now discuss the origin of the buckling at the kink, which explains the formation of the intrinsic structure near the kinks such as the $p(2\times2)$ and the buckling of dimers of a rebonded dimer row (RDR) as shown in Fig. 4. As a starting point of the discussion, the structure of the S_A step is taken into account. The S_A step forms at the exposed side of the S_B step naturally. Since the dimers of the S_A step are buckled as discussed previously, the dimer at the kink has to be buckled. At the kink, the asymmetric effect is substantial because two sides are open. It induces a large buckling of the

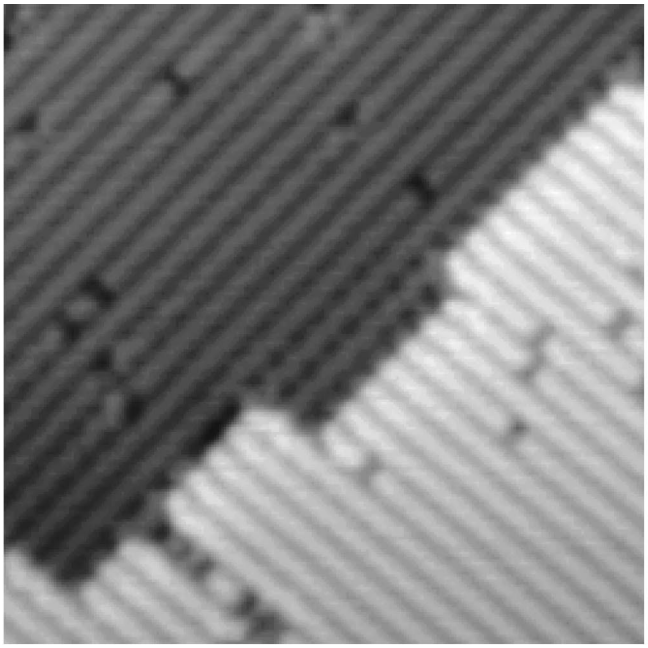

(a)

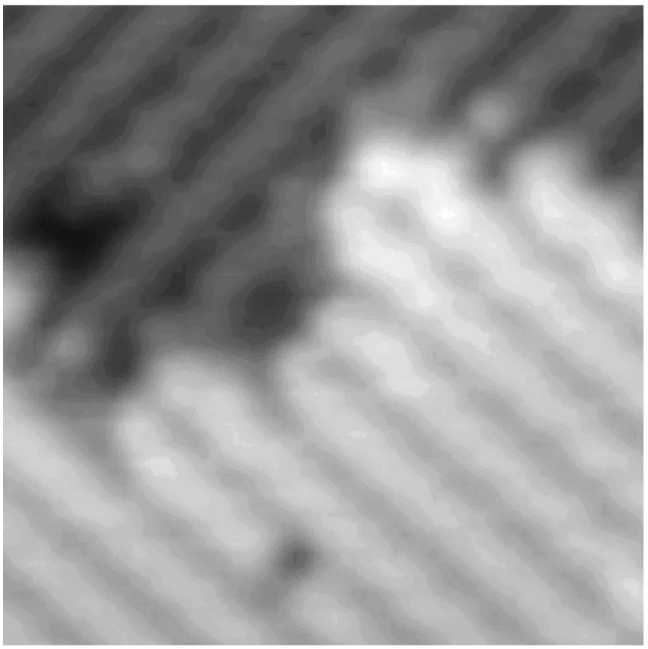

(b)

FIG. 3. (a) Filled-state STM image of the S_B step on the Si(001) surface. The basic S_B step edges are terminated with rebonded dimers. The dimers at the kinks are directed toward the center of the S_B step irrespective of the type. The P kink induces a strong zigzag buckling along the dimer row in the lower terrace. (b) The narrow S_B step with only two dimer rows forms a local $c(4\times2)$ structure.

kink dimer compared to that of other rebonded dimers of the S_B step.

Figure 4(a) shows the typical structure near a P kink of a monatomic step on the Si(001) surface. The terminating dimer AB at the P kink is rebonded and is aligned with the gap between two dimer rows in the lower terrace. Since the outmost dimer row containing the dimer AB in Fig. 4(a) makes an S_A step and the configuration of the S_A step as

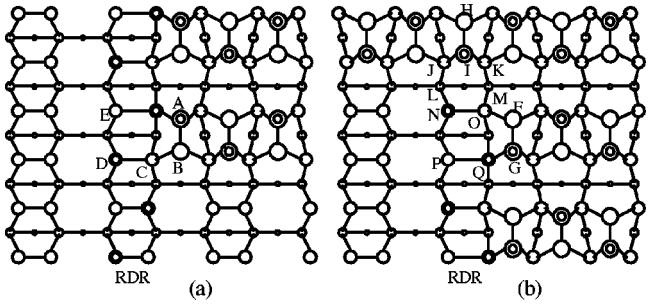

FIG. 4. (a) Schematic atomic structure near a P kink of monatomic steps on the Si(001) surface. The two dimer rows near the P kink form a local $p(2\times2)$ structure to retain the zigzag buckling of the RDR. (b) Structure near an N kink. The dimer FG at the N-kink site is buckled to form a local $c(4\times2)$ structure together with the outer longer dimer row.

represented in the figure is energetically stable against the other variant, the dimer AB is buckled in such a way that the atoms A and B are buckled upward and downward, respectively. It explains the reason why the dimer at the P kink is buckled toward the center of the S_B step in the filled-state STM image.

Then the downward buckled atom B makes the atom C rotate by pushing down the bonding BC at the P kink of Fig. 4(a). The downward strain of the bonding BC again pushes up the atom D to retain the sp^3 bonding character of the atom C. By the same logic the upward buckling of atom A makes the atom E downward. Since the buckling is substantial at the kink, other dimers on the RDR adjust themselves to meet the condition of the zigzag buckling of the RDR. For the case of a wide S_B step, the inner dimer row of the upper terrace near the P kink builds a local $p(2\times2)$ structure together with the outermost dimer row to retain the zigzag buckling of the RDR. Provided that a local $c(4\times2)$ forms, the configuration should violate the zigzag buckling of the RDR. However, the structure has not been observed in a wide S_B step on the well-prepared Si(001) surface, showing that the condition of zigzag buckling of the RDR is strong enough to compensate for the total energy gain due to the formation of the $p(2\times2)$ structure on the upper terrace near the P kink. This zigzag buckling of the RDR extends far in the lower terrace as shown in Figs. 3(a) and 3(b).[20]

Figure 4(b) shows an atomic configuration near the N kink. Our experiment in Fig. 3(a) shows that the buckling of the dimer at the N kink is larger than that of the inner rebonded dimers at the S_B step edge and is directed toward the center of the S_B step in the filled-state STM image. The outer longer dimer row located at the neighbor of the N kink forms a S_A step and stabilizes the unique strong buckling by itself. The outermost dimer row terminating at the N kink constructs a local $c(4\times2)$ structure together with this outer longer dimer row. This local $c(4\times2)$ structure comes from the buckling of the dimer FG at the N kink in Fig. 4(b). The strong buckling of the dimer HI and neighboring dimers on the same dimer row in Fig. 4(b) is expected because of a substantial asymmetric effect of the S_A step edge. It causes a large distortion of the atoms J and K toward the atom I. Under this condition the atoms N and O are distorted in such a way that the lateral distance between N and O is shorter than that between atoms P and Q. This distortion of the

atoms N and O is induced to reduce the strain energy of the atoms L and M in the third layer in the same manner as in Fig. 2. The difference in strains exerted between the atoms O and Q induces the buckling of the dimer FG such that atoms F and G are buckled downward and upward, respectively. Therefore, the dimer at the N-kink site is also buckled toward the center of the S_B step, whose origin is different from that at the P kink. It explains the reason why the dimer at the N kink is also buckled toward the center of the S_B step as in Fig. 3(a).

The inner rebonded dimer at the wide S_B step edge is buckled in the same direction as the dimer FG at the N-kink site by the influence of the zigzag buckling of the RDR, inducing the local $p(2\times2)$ structure as the case near the P kink. The interaction of the dimer at the N kink with the outer S_A step edge is strong enough to break the zigzag buckling of the RDR near the center of the S_B step segment as shown in Fig. 3(b).

In conclusion, the kinked monatomic step structure on the Si(001) surface is investigated by scanning tunneling microscopy. The bonding configuration and strain of the broken dimer rows at the S_B step edge are responsible for the construction of the various structures observed near the S_B step. The S_A and S_B steps are structurally correlated through the kinks and the reconstruction pattern near the S_B step is determined by the buckling of the S_A steps through the subsurface interaction.

This work was supported by the Ministry of Science and Technology of Korea and in part by the Korea Science and Engineering Foundation through the ASSRC at Yonsei University. J.-Y. Yi acknowledges support from the Ministry of Education, Republic of Korea, Project No. BSRI-97-2412.

*Author to whom correspondence should be addressed. Fax: +82-42-868-5027. Electronic address: koojayon@kriss.re.kr

[1] R. M. Tromp, R. J. Hamers, and J. E. Demuth, Phys. Rev. Lett. **55**, 1303 (1985); R. J. Hamers, R. M. Tromp, and J. E. Demuth, Phys. Rev. B **34**, 5343 (1986).
[2] J.-Y. Koo, J.-Y. Yi, C. Hwang, D.-H. Kim, S. Lee, and D.-H. Shin, Phys. Rev. B **52**, 17 269 (1995).
[3] A. Garcia and J. E. Northrup, Phys. Rev. B **48**, 17 350 (1993).
[4] J. Dabrowski, E. Pehlke, and M. Scheffler, Phys. Rev. B **49**, 4790 (1994).
[5] D. J. Chadi, Phys. Rev. Lett. **43**, 43 (1979).
[6] M. Tsuda, T. Hoshino, S. Oikawa, and I. Ohdomari, Phys. Rev. B **44**, 11 241 (1991).
[7] R. A. Wolkow, Phys. Rev. Lett. **68**, 2636 (1992).
[8] H. Tochihara, T. Amakusa, and M. Iwatsuki, Phys. Rev. B **50**, 12 262 (1994).
[9] D. Badt, H. Wengelnik, and H. Neddermeyer, J. Vac. Sci. Technol. B **12**, 2015 (1994).
[10] P. Boguslawski, Q.-M. Zhang, Z. Zhang, and J. Bernholc, Phys. Rev. Lett. **72**, 3694 (1994).
[11] K. C. Low and C. K. Ong, Phys. Rev. B **50**, 5352 (1994).
[12] J. Fritsch and P. Pavone, Surf. Sci. **344**, 159 (1995).
[13] D. J. Chadi, Phys. Rev. Lett. **59**, 1691 (1987).
[14] P. E. Wierenga, J. A. Kubby, and J. E. Griffith, Phys. Rev. Lett. **59**, 2169 (1987).
[15] O. L. Alerhand, A. N. Berker, J. D. Joannopoulos, D. Vanderbilt, R. J. Hamers, and J. E. Demuth, Phys. Rev. Lett. **64**, 2406 (1990).
[16] B. S. Swartzentruber, Y.-W. Mo, R. Kariotis, M. G. Lagally, and M. B. Webb, Phys. Rev. Lett. **65**, 1913 (1990).
[17] B. S. Swartzentruber, Y. W. Mo, M. B. Webb, and M. G. Lagally, J. Vac. Sci. Technol. A **8**, 12 262 (1990).
[18] F. Wu, S. G. Jaloviar, D. E. Savage, and M. G. Lagally, Phys. Rev. Lett. **71**, 4190 (1993).
[19] J.-Y. Koo, J.-Y. Yi, C. Hwang, D.-H. Kim, S. Lee, and J. Cho, Phys. Rev. B **54**, 10 308 (1996).
[20] H. Tochihara, T. Sato, T. Sueyoshi, T. Amakusa, and M. Iwatsuki, Phys. Rev. B **53**, 7863 (1996).